RELATIONSHIP BETWEEN CRANIAL BASE DEVELOPMENT AND CLEFT LIP AND PALATE IN *PRICKLE1* BEETLEJUICE MUTANT: CASE CONTROL STUDY

by

Eunsol Victoria Lee

B.Sc. in Chemistry, Rutgers University, 2012

D.D.S., New York University, 2017

Submitted to the Graduate Faculty of

School of Dental Medicine in partial fulfillment

of the requirements for the degree of

Master of Dental Science

University of Pittsburgh

2020

UNIVERSITY OF PITTSBURGH

SCHOOL OF DENTAL MEDICINE

This thesis/dissertation was presented

by

Eunsol Victoria Lee

It was defended on

Select the Date

and approved by

Dr. Yong Wan, Research Assistant Professor, Department of Medicine

Dr. J. Matthew Stacy Jr., Clinical Assistant Professor, Department of Orthodontics & Dentofacial Orthopedics

Thesis Director: Dr. Heather Szabo-Rogers, Assistant Professor, Department of Oral Biology

RELATIONSHIP BETWEEN CRANIAL BASE DEVELOPMENT AND CLEFT LIP AND PALATE IN PRICKLE1 BEETLEJUICE MUTANT

Eunsol Victoria Lee, DDS, MDS

University of Pittsburgh School of Dental Medicine, 2020

Cleft lip and/or palate (CL/P) is one of the most common congenital anomalies in United States. Its etiology is complex, multifactorial, and not well understood. This study focuses on *Prickle1 Beetlejuice (BJ)* mutants which tend to have compressed and wide facial morphology. *Prickle1* is a core component of Wnt/Planar cell polarity(PCP) pathway and the *Prickle1*^{Bj} mouse line has a missense mutation (p.Cys161Phe) that disrupts the LIM1 domain in *Prickle1*. These mutants have approximately 50% chance of developing a cleft palate. Because cranial base size and shape determine the perimeter of growth for the lower 2/3 of the face, we examine the association between cranial base development and orofacial cleft. We found that *Prickle1*$^{Bj/Bj}$ with cleft lip and/or palate have wider, shorter, and less dense basisphenoid compared to wild type. Mutants with both cleft lip and palate compared to mutants with cleft lip only have even shorter and less dense basisphenoid. However, the basisphenoid width difference between the mutant groups was not statistically significant. Our data supports the conclusion that wide basal cranium poses higher risk of developing orofacial cleft. Yet, basisphenoid bone density is the superior value in determining the degree of orofacial cleft.

TABLE OF CONTENTS

LIST OF TABLES

LIST OF FIGURES

PREFACE

I would like to thank Dr. Heather Szabo-Rogers, Dr. Yong Wan, and Lyudmila Ivantayeva-Lukashova (School of Dental Medicine University of Pittsburgh) for guidance and technical assistance.-=

1.0 INTRODUCTION

Orofacial clefts are one of the most common types of birth anomalies. In United States each year, about 4,440 infants are born with a cleft lip with or without a cleft palate (Parker et al 2010). The etiology is unknown, but it is multifactorial including genetics, environmental, geographic, racial and ethnic, and socioeconomic status (Grosen et al 2010, Dixon et al 2011). Clefting of the lip occurs because of a failure of fusion between the medial nasal processes and the maxillary prominences. Cleft palate is a result of incomplete closure of the secondary palate by elevation of the palatal shelves (Proffit et al 2007). Orofacial cleft is not life-threatening, but may affect functions such as feeding, digestion, speech, middle-ear ventilation, hearing, respiration and facial and dental development (Ferguson et al 1988, Christensen et al 2004). The emotional stress that accompanies CL/P patients and their families can be life changing. This issue was highlighted in a study stating that 30% of mothers of children with CL/P have contemplated suicide (Natsume et al 2013). Treatment with multiple surgeries throughout a patient's life is a financial burden for both families and US health care industry. CDC estimated that health care industry invests about $679 million per year in treating CL/P patients (National Institute of Dental and Craniofacial Research 2018). Thus, it is imperative to broaden our understanding of orofacial clefts. There are many theories regarding the development of cleft palate, but not enough evidence is presented on why palatal shelves fail to integrate after elevation. This study concentrates on developmental contribution to palatal cleft.

1.1 PALATOGENESIS

To appreciate molecular mechanism behind cleft palate, one must understand the process of normal palatal development, known as palatogenesis. The embryologic development of the primary palate begins very early in gestation and the upper lip and primary palate have usually fused by the seventh week of gestation (Gleason et al 2018). It becomes established as the medial nasal and maxillary processes fuse, failure or incomplete fusion leads to cleft lip development. The secondary palate originates as an outgrowth of the maxillary prominences at approximately embryonic day 11.5 in the mouse and six weeks in humans. The palatal shelves initially grow vertically from each side of the maxillary arch along the sides of the tongue. The lower part of the developing face, encompassing the tongue and the floor of the oral cavity, becomes displaced downward and forward due to the growth of the mandible. Then the shelves rise above the tongue, and "swing upward" in order to contact each other. With continued growth, the shelves apposing at the midline eventually fuse, forming the secondary palate. (Enlow et al 2008, Murray et al 2004). Following palatal shelf elevation, epithelial cell proliferation allows the middle edge epithelium (MEE) of the two palatal shelves to approximate each other at the midline. Once the palatal shelves make contact, MEE reduces to create a single-layered midline epithelial seam (MES). The MES subsequently disintegrates to allow for mesenchymal confluency in a process termed palatal fusion. There are three primary cellular mechanisms thought to be responsible for palatal shelf fusion: epithelial cell apoptosis, migration and transition to the mesenchymal state via the epithelial-to-mesenchyme transition (EMT) process. (Nawshad 2008, Bush et al 2012). Any disruption in these stages may cause a cleft palate.

1.2 NASOMAXILLARY COMPLEX IN RELATION TO CRANIAL BASE

The basicranium dimension determines a person's facial form which affect proportionate and topographic features of the lower 2/3 of the face. Individuals with a dolichocephalic head shape have a brain that is long in the anteroposterior direction and narrow in the transverse direction (Franco et al 2013). Dolichocephalic patients tend to have a more elongate and open-angle configuration (Enlow et al 2008). On the other hand, patients who are brachycephalic have rounder, wider, and anterioposterioly shorter cranial base (Franco et al 2013). They characteristically have a retrusive nasomaxillary complex and vertically short skeletal relationship (Enlow et al 2008). Orthodontists come to understand that basicranium serves as the template that establishes the shape and perimeter of the facial growth field (Enlow et al 2008).

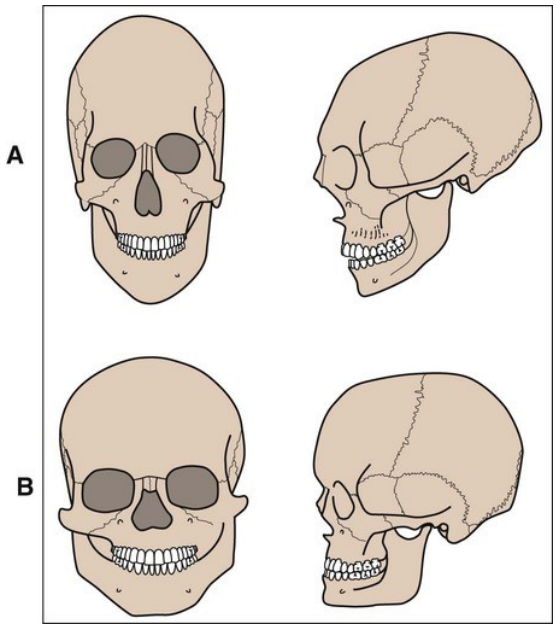

Figure 1.1 Cranial base shape A) Dolichocephalic head form B) Brachycephalic head form
Kuroda, Shingo. Facial Growth and Development. *Pocket Dentistry.* 5 Jan. 2015, https://pocketdentistry.com/14-facial-growth-and-development/

The reason why one's midface is directly influenced by their basicranium shape is because anatomically, nasomaxillary complex is situated beneath the anterior cranial fossa. The anterior boundary of the skull corresponds to the anterior border of the nasomaxillary complex, and the posterior plane of the midface extends from the junction between the anterior and middle cranial fossa (Enlow et al 2008). Laterally maxilla is bound zygomatic bones which is also connected to the skull by sphenoid, temporal, and frontal bones. The perimeter and growth of the midface is, therefore, directly influenced by the floor of the cranium (Enlow et al 2008).

1.3 DEVELOPMENT AND TISSUE ORIGINS OF THE MAMMALIAN CRANIAL BASE

The mammalian cranial base is a complex structure composed of bone, cartilage, and connective tissue. Cranial base is the floor of the braincase and is comprised of ethmoid, presphenoid, basisphenoid, and basioccipital bones formed by endochondral ossification. The chondrocranium develops between E11 and E16 in the mouse, beginning with caudal (occipital) chondrocranium, followed by rostral structures. Final fusion of these parts occurs via a midline stem and lateral struts by E16 (McBratney-Owen et al 2008). Studies have demonstrated that neural crest cells contribute to most of the cartilages in the anterior region of the skull (ethmoid, presphenoid, and basisphenoid). Posterior region (basioccipital and non-squamous parts of the temporal bone) is mesoderm derived (McBratney-Owen et al 2008).

1.4 TYPES OF PALATAL CLEFT

1.4.1 FAILURE OF PALATAL SHELF FORMATION

Failure of palatal shelf formation is a rare condition. Recent findings identified multiple molecular components that are necessary between the palatal shelf epithelium and mesenchyme during palatogenesis. These networks include signaling molecules and growth factors such as sonic hedgehog (Shh), transforming growth factor β (TGf β), bone morphogenetic proteins (Bmps) and fibroblast growth factors (Fgfs) (Murray et al 2004). Fgf10-/- mutants were found with altered cell proliferation within mesenchyme and epithelium in the palatal shelves and increased apoptosis in the epithelium, thus affecting the initial development of palatal shelves.

(Rice et al 2004) In addition, other genes, including Msx1, Lhx8, Shox2, and Osr2, are known to have key roles in the palatal shelf growth. When the targeted mutation of these genes and defect in molecular components generate cleft palate, it is an indication that intrinsic factors are required in palatogenesis (Yu et al 2005).

1.4.2 FUSION OF THE PALATAL SHELF WITH OTHER STRUCTURES

In normal growth and development, palatal shelves only fuse to each other. However, in mice that do not express Fgf10, the palatal shelf epithelium fuses with the tongue and mandible (Rice et al 2004). Thus, the elevation of palatal shelf becomes inhibited.

1.4.3 FAILURE OF PALATAL ELEVATION

Palatal shelf elevation is a fast movement influenced by both intrinsic forces and developing craniofacial and oral structures, such as downward displacement of the tongue, and growth of the cranium and mandible. (Ferguson 1988). Recent studies indicate that extracellular matrices play a key role in palatal shelf closure. It is suggested that posterior palatal shelf remodeling is largely from expansion of hyaluronate network within the mesenchymal compartment (Brinkley et al 1984). Mutations of Pax9, Pitx1 or Osr2 are also known to cause failed palatal shelf elevation (Kist et al 2007, Szeto et al 1999, Gao et al 2009). Defective γ-Aminobutyric acid (GABA), a major inhibitory neurotransmitter, also generate cleft palate by inhibiting palatal shelf elevation (Ding et al 2004).

1.4.4 PERSISTENCE OF MIDDLE EDGE EPITHELIUM

Adhesion of the opposing middle edge epithelium (MEE) is an important step in formation of the palate. Epithelial-mesenchymal transition (EMT) is the current proposed mechanism that regulates disappearance of MES to generate mesenchyme continuity (Nawshad et al 2004). Tgfβ3 signaling functions to mediate EMT, and without it, mutant mice are born with MEE that fail to undergo apoptosis (Kaartinen et al 1995, Miettinen et al 1999).

1.4.5 EARLY OSSIFICATION OF THE PALATE

Many studies confirmed that fusion of the palatal shelves along the mid-palatal suture occurs during the ossification of the maxillae and palatine bones. If ossification of the palate occurs too early, it may result in a pathological cleft. *Sox9* is a gene controlling cartilage development and suppressing the expression of *Runx2*, a transcription factor for osteoblast differentiation and bone formation. In *Sox9* mutants, *Runx2* is no longer repressed and ossification begins prematurely. As a result, palatal shelves are prematurely ossified, and they cannot grow toward the midline to fuse (Mori-Akiyama et al 2003).

1.4.6 FAILURE OF PALATAL SHELVES TO MEET AFTER ELEVATION

During fusion, the epithelium covering the tip of the opposing palatal shelves adhere and intercalate into a single-layer medial edge epithelial seam (MES). The dismantling of this seam results in the convergence of palatal mesenchyme (Nawshad 2008). When this process is disrupted, palate fails to integrate properly. Failure of shelf fusion is the most common type of cleft palate defect documented in animal studies. Current known causes of this condition are

mutations in *Msx1* and *Lhx8*, and inactivation of *Tgfbr2* in cranial neural crest cells or *Shh* in the epithelium (Rice et al 2004).

1.5 PLANAR CELL POLARITY

Wnt/Planar cell polarity (PCP) is a conserved pathway that plays a crucial role in development. It allows polarization of cells within an epithelial sheet, orthogonal to the apical-basal polarity axis. Core PCP proteins are Van Gogh/Strabisumus, Prickle, Frizzled, Dishevelled, Diego, and Flamingo (Devenport 2014, Vladar et al 2009). These proteins accumulate asymmetrically at proximal and distal apical cell junctions, creating cell polarity along the forming tissue axes (Axelrod et al 2014). Disruption in this process causes many possible developmental anomalies, including the misalignment of hair cells in the cochlea, neural tube closure, brain and skeletal defects, and congenital heart disease (Cui et al 2013).

Wnt signaling has been shown to regulate convergent-extension (CE) and is required for palate extension in the anteroposterior and transverse axes (Rochard et al 2016). CE can be described in three steps: cells proliferate and aggregate distally at the newly formed part of the palate, cells mature and organize into columns, and finally the chondrocytes intercalate proximally and drive elongation in the AP axis while remaining as a single cell layer in the dorsoventral axis (DV). *Wntless (wls)* mutants were found with smaller and rounder chondrocytes that lacked stacking in linear columns. Chondrocytes did not intercalate with neighboring cells and were randomly oriented, exhibiting excessive stacking in the dorsoventral axis (Rochard et al 2016). Therefore, without proper regulation of planar cell polarity, there is a high risk of orofacial cleft pathogenesis.

1.6 *Prickle1 (PK1)*

Prickle1 (PK1) is a negative regulator of the Wnt/β-catenin and Wnt/PCP signaling pathway. Defective *PK1* has been found to result in early maturation and stalling of terminal differentiation of chondrocytes, and depolarization of PCP proteins (Wan et al 2018). Disruption in core PCP proteins *Prickle1a* or *Prickle1b* causes pre-migratory cranial neural crest cells (NCCs) to cluster together at the dorsal end of the neural tube, where they adopt aberrant polarity and movement. NCCs also fail to complete epithelial-to-mesenchymal transition (EMT) (Ahsan et al 2019). Phenotypically, *Prickle1* mouse mutants exhibit midfacial hypoplasia and shortened limbs (Gibbs et al 2016, Wan et al 2018). Their skull is compressed in the AP axis while expanded in the transverse axis (Wan et al 2018).

1.7 OBJECTIVE OF STUDY

The aim of this study are: 1) to characterize the development of cranial base in *Prickle1*$^{Bj/Bj}$ mice; 2) to determine whether there is an association between cranial base development and orofacial cleft. Since basicranium serves as the template and perimeter for growth in the lower 2/3 of the face, it seems plausible that a wide cranial base contributes to a longer distance for developmental processes to travel before fusing. Thus, a wide basicranium may increase the risk of developing orofacial cleft. Our hypothesis is that defective Prickle1 protein will result in a wide cranial base, subsequently creating an orofacial cleft.

2.0 MATERIALS AND METHODS

In this study, we focus on *PK1* missense allele, named *Beetlejuice (Bj)*. *Beetlejuice* mutants only survive to term while displaying wide spectrum of developmental anomalies such as congenital heart defect, skeletal and craniofacial anomalies, and cochlea defects (Gibbs et al 2016). We sampled 10 mice, 6 mutants and 4 littermate controls at stage E17.5. Four of the mutants developed cleft lip while two of the mutants had both cleft lip and palate. We excluded heterozygous mice. Animal care and use were complied with the guidelines of Institutional Animal Care and Use Committee of University of Pittsburgh.

2.1 EMBRYO COLLECTION AND GENOTYPING

For timed matings, the day the plug was observed was designated E0.5. At E.17.5, embryos were collected by C-section after euthanasia of pregnant mice. Staging was confirmed by morphology. All the embryos and fetuses were placed in 4% paraformaldehyde overnight and embedded in paraffin using standard protocol. Genotyping was established by using Taqman SNP assay (Invitrogen, AH7041R), Taqman genotyping master mix, and IMPLEN Nanophotometer (Wan et al 2018)

2.2 MICROCOMPUTED TOMOGRAPHY AND ANALYSIS

Previous to microCT scan, mice were fixed in 95% ethanol and mandible was removed. Scanco μCT50 was used for imaging. Obtained scans were oriented to superior endocranial view

for imaging and measurements. Basisphenoid (BS) and basioccipital (BO) are utilized for measurements because they are well developed and easy to visualize by E17.5. Each bone's width, length, BV/TV, and bone mineral density (BMD) are analyzed. BV/TV stands for Bone Volume over Total Volume, measured in percentage. BMD is an actual measure of the amount of minerals contained in a certain volume of bone. Dimensions of width and length for each bone is described in Table 2.1 and Figure 2.1. Some of the landmarks are provided by Richtsmeier laboratory at The Pennsylvania State University (www.biteit.org).

Table 2.1. Dimensions of Width and Length

Bone	Measurement	Dimension
Basisphenoid (BS)	Width	Most postero-lateral points
	Length	Vertical line from AMSPH
Basioccipital (BO)	Width	LSYN to RSYN
	Length	Vertical line from BAS

AMSPH, LSYN, RSYN, and BAS are landmarks obtained from Richtsmeier Laboratory at The Pennsylvania State University. AMSPH - Most antero-medial point on the body of the sphenoid. LSYN - Most antero-lateral point on the corner of the basioccipital, Left side. RSYN - Most antero-lateral point on the corner of the basioccipital, Right side. BAS - Mid-point on the anterior margin of the foramen magnum, taken on basioccipital.

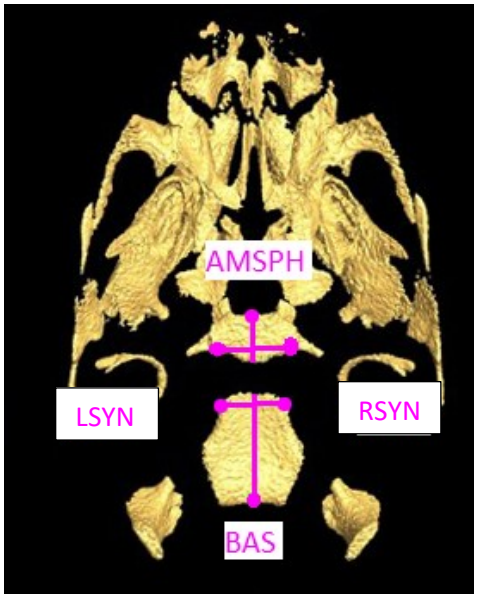

Figure 2.1 Dimensions of Width and Length Measurements

2.3 HISTOLOGICAL ANALYSIS

For histomorphometry, mice were stained with Alcian Blue/Alizarin Red. Samples fixed in 95% ethanol were transferred to acetone overnight to remove fat. After rinsing with deionized water, Alcian Blue stain was applied for 24 hours to visualize cartilage. Washing was completed with 70% ethanol for 6-8 hours then samples remained in 1% potassium hydroxide until tissues were visibly cleared. Bones were counterstained with Alizarin Red overnight. Samples were placed in 1% potassium hydroxide / 20% glycerol solution for 2 days. Finally, mice were stored and imaged in glycerol:ethanol (1:1).

2.4 CELL POLARITY ANALYSIS

Two (*Prickle1*$^{Bj/Bj}$ *Prickle1*$^{+/+}$) littermates are stained with DAPI and BrdU. Coronal section slides were made for visualization. 4',6-diamidino-2-phenylindole (DAPI) is a fluorescent stain that labels DNA and allows for easy detection of nucleus in interphase cells and chromosomes in mitotic cells (Chazotte 2010). BrdU is a thymidine analog that incorporates into the DNA of proliferating cells in S phase. Rapidly dividing or transit amplifying cells can dilute or lose the BrdU label upon multiple cell divisions (Lei et al 2015). BrdU labelled cells can be detected by a primary antibody that detects BrdU. Cells stained with both DAPI and BrdU are analyzed, and the angle between two dividing cells is measured with Image J. Data is summarized in polar graph and polar histogram.

2.5 STATISTICAL ANALYSIS

Data was compared and analyzed using the Student's *t*-test between *Prickle1*$^{Bj/Bj}$ and *Prickle1*$^{+/+}$ littermates. Additional t-test was performed between mutants with cleft lip only vs. mutants with cleft lip and palate. Scattered plot and linear regression are applied to determine if there is a trend as one progresses from wild type, mutant with only cleft lip to mutant with both cleft lip and palate. A *p*-value of <0.05 was considered significant. All analyses were performed using StataSE 15 software.

3.0 RESULTS

3.1 MORPHOLOGY OF THE E17.5 CRANIAL BASE

3.1.1 ALCIAN BLUE and ALIZARIN RED STAINING

To determine the cranial base morphology we collected the embyros and stained them with alcian blue and alizarin red to visualize bone and cartilage respectively. In the cranial base, the basioccipital is similar between *Prickle1*$^{Bj/Bj}$ and *Prickle1*$^{+/+}$ control animals (Fig 3.1). Malformation was detected in both the basisphenoid and presphenoid. The *Prickle1*$^{Bj/Bj}$ presphenoid bone consisted of two small and faint structures joined by a bridge of tissue. The *Prickle1*$^{+/+}$ control showed one, well defined, unified structure. The *Prickle1*$^{Bj/Bj}$ basisphenoid bone also had a discontinuity in the midline.

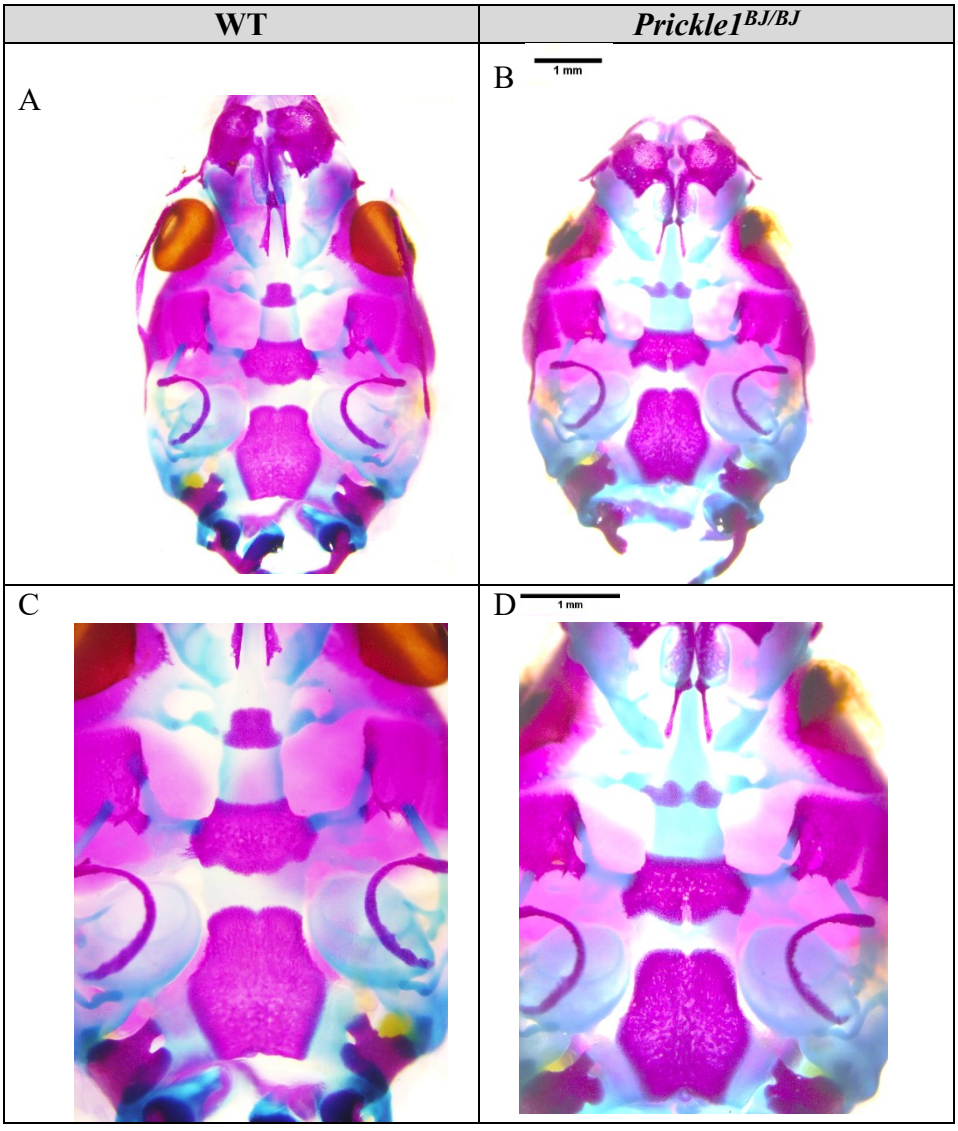

Figure 3.1 Cranial base staining. Cranial base comparison between wild type and *Prickle1*$^{BJ/BJ}$ mice. A,B) Alcian blue (cartilage) and Alizarin red (ossified bone) staining of E17.5 WT (left) and *Prickle1*$^{BJ/BJ}$ (right) mouse heads in 1.6x magnification. Inferior view of skull displaying malformation of presphenoid and deficient bone density in the midline structure of basisphenoid in *Prickle1*$^{BJ/BJ}$ mice. C) Sample A in 2.5x magnification. D) Sample B in 2.5x magnification.

3.1.2 MICROCT IMAGES

After observing bone morphology differences using alizarin red staining, I hypothesized that the bone mineral density may be affected in the *Prickle1*$^{Bj/Bj}$ mutants. We performed high resolution micro CT scans. The μCT scans revealed the same midline discontinuities and revealed that the *Prickle1*$^{Bj/Bj}$ bones had greater porosity suggestive of a problem with mineralization (Fig. 3.2).

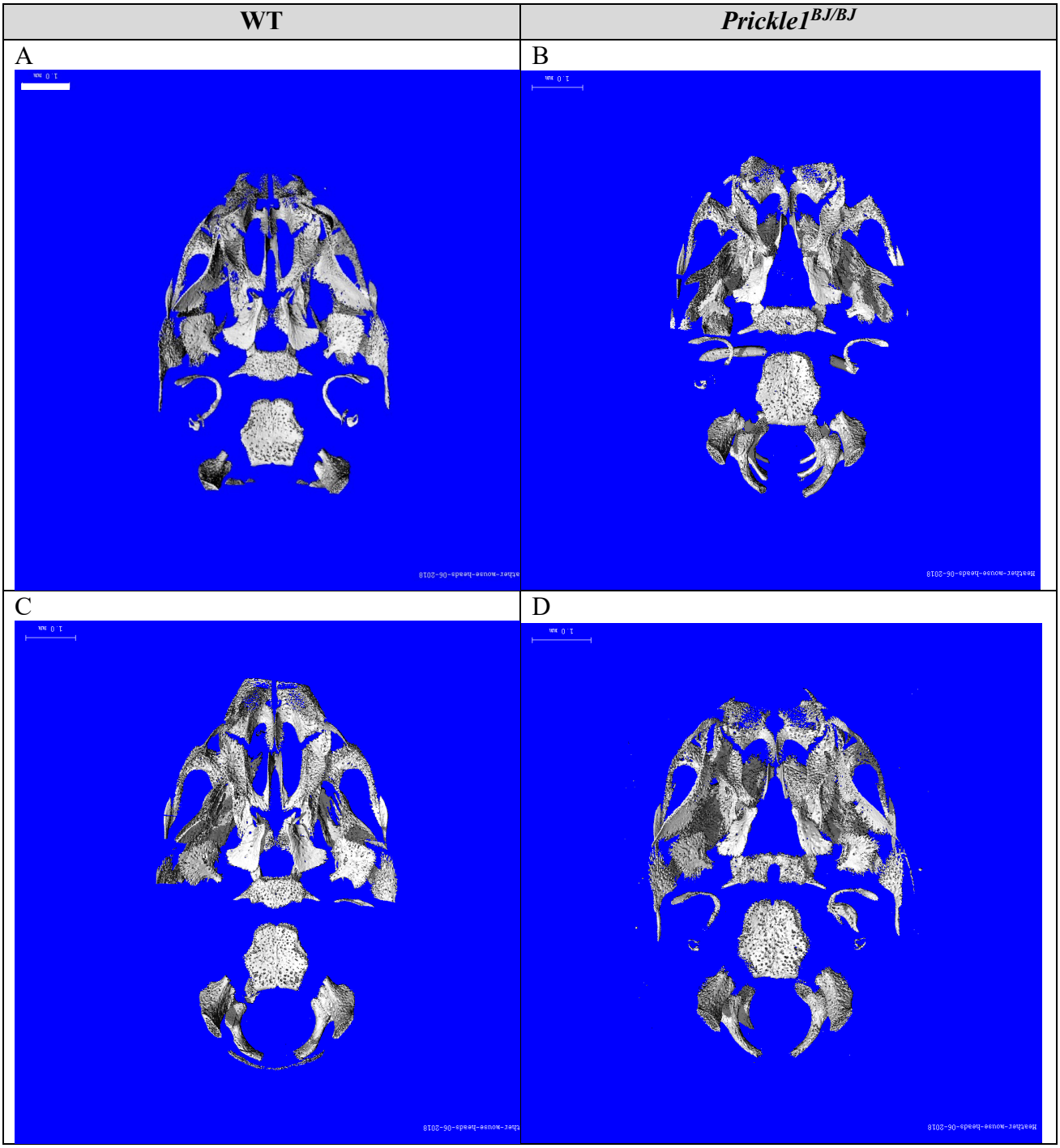

Figure 3.2 MicroCt Imaging A,C) Endocranial view of WT microCT. B) Endocranial view of Cleft Lip only *Prickle1*$^{BJ/BJ}$ microCT. Increased porosity at the midline of basisphenoid D) Endocranial view of Cleft Lip and Palate *Prickle1*$^{BJ/BJ}$ microCT. Failure of fusion at the midline of basisphenoid.Scale bar in A = 1.0mm, and it applies to B-D

3.2 BASISPHENOID and BASIOCCIPITAL MEASUREMENTS

Using both the alizarin red, and μCT images I observed that the width of the basisphenoid seems to be wider in the *Prickle1*$^{Bj/Bj}$ mutants. To test this hypothesis, I performed an analysis where I measured the width, length, BV/TV, and BMD of the basisphenoid and basioccipital of the *Prickle1*$^{Bj/Bj}$ mutants and controls. I compared the measurements using paired t-test in StataSE 15 software.

Paired t-test demonstrated that there was a statistically significant difference in basisphenoid's width, length, BV/TV, and BMD between mutants and wild type. The results display the difference in mean value and standard deviation. None of the confidence interval include zero, indicating a difference in the groups. These results are found in Table 3.1.

Table 3.1: **Comparison of the Means (t-test) Basisphenoid**

Basisphenoid	Genotype	Mean	Std. Dev.	95% Conf. Interval		P-Value
Width	Wild Type	1.10675	.0356406	1.050038	1.163462	0.0027**
	Mutant	1.244	.0511957	1.180432	1.307568	
Length	Wild Type	.67725	.0501955	.5973778	.7571222	0.0499*
	Mutant	.6064	.03996	.5567831	.6560169	
BV/TV	Wild Type	.403225	.0182063	.3742547	.4321953	0.0080**
	Mutant	.31124	.0468764	.2530353	.3694447	
Actual Density (BMD)	Wild Type	1.662875	.0175148	1.635005	1.690745	0.0031**
	Mutant	1.50592	.0685782	1.420769	1.591071	

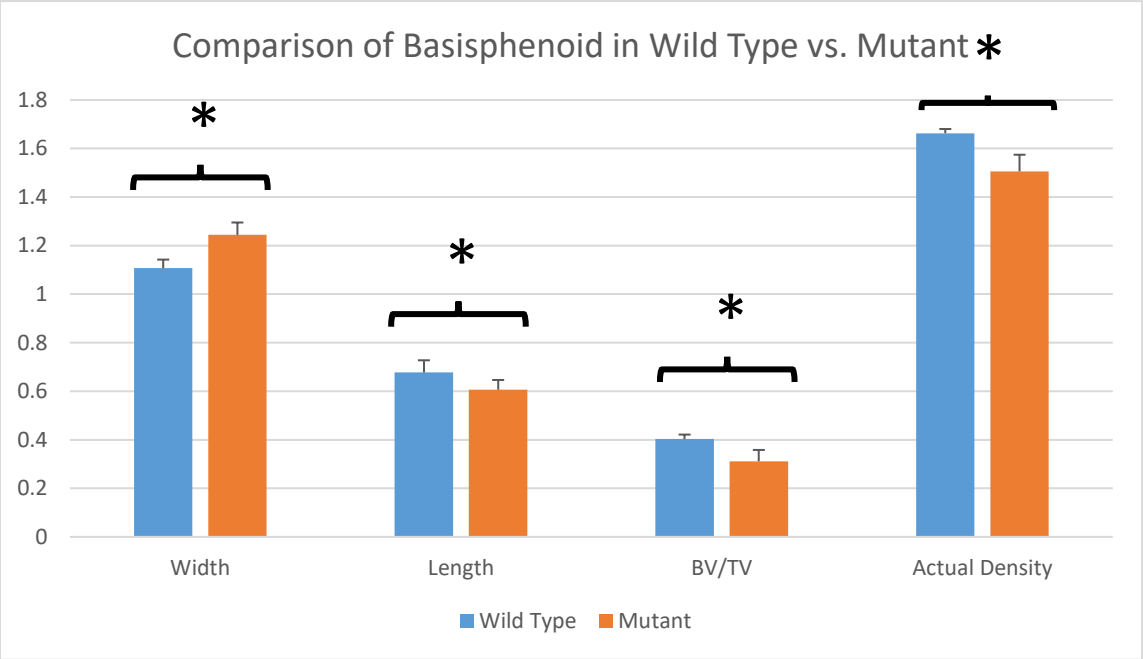

Figure 3.3: **Basisphenoid Comparison between Wild Type vs. Mutant**

Paired t-test demonstrated there was no statistical difference in basioccipital width, length, BV/TV, and BMD between mutants and wild type. The results display the difference in mean value and standard deviation. None of the confidence interval include zero, confirming the lack of a difference between two groups. These results are found in Table 3.2.

Table 3.2: Statistical analysis of Basioccipital bone

Basioccipital	Genotype	Mean	Std. Dev.	95% Conf. Interval		P-Value
Width (mm)	Wild Type	.858	.054827	.770758	.945242	0.8646
	Mutant	.8634	.0370176	.8174366	.9093634	
Length (mm)	Wild Type	1.52425	.1288601	1.319205	1.729295	0.4053
	Mutant	1.5796	.0523431	1.514607	1.644593	
BV/TV (%)	Wild Type	.411175	.0150504	.3872264	.4351236	0.1363
	Mutant	.37458	.0408602	.3238453	.4253147	
Actual Density (g/cm2)	Wild Type	1.77455	.0255323	1.733922	1.815178	0.0740
	Mutant	1.65358	.1114966	1.515139	1.792021	

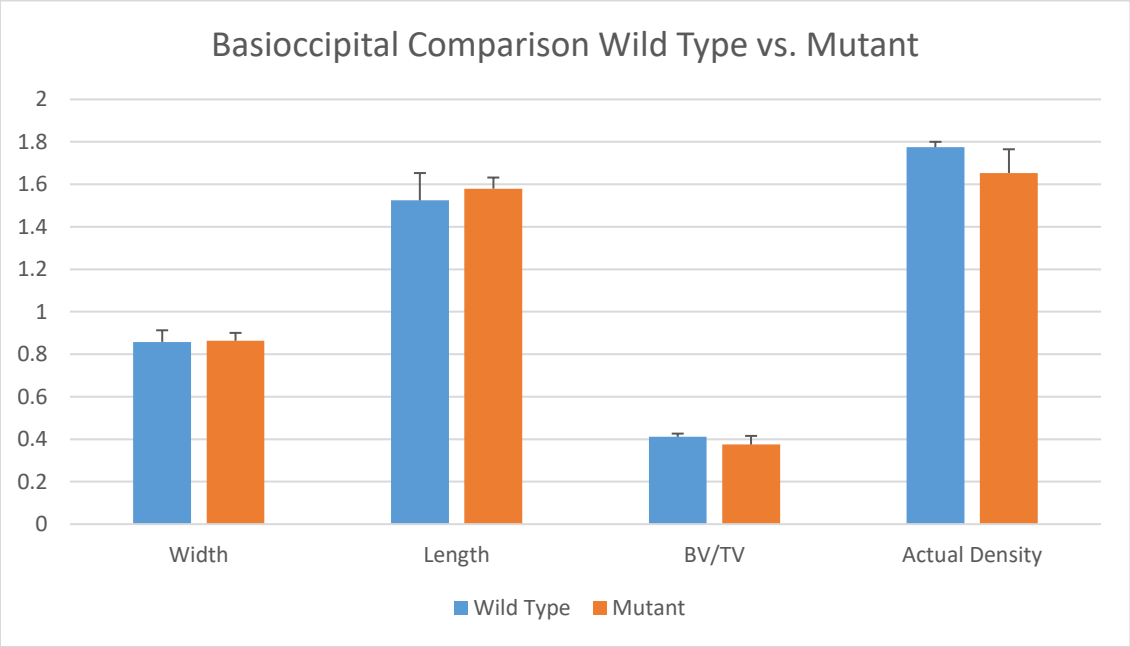

Figure 3.4: Basioccipital Comparison between Wild Type vs. Mutant

3.3 BASISPHENOID COMPARISON IN CLEFT LIP ONLY VS. CLEFT LIP AND PALATE

I hypothesized that the *Prickle1*$^{Bj/Bj}$ animals that developed both cleft lip and palate may have wider basisphenoid compared to the *Prickle1*$^{Bj/Bj}$ with isolated cleft lip. My hypothesis stems from the anatomical relationship of nasomaxillary complex to the cranial base. As cranial base widens, I expected the degree of clefting to worsen from cleft lip only to both cleft lip and palate.

In Table 3.3, a separate t-test is performed to compare width, length, BV/TV, and BMD of basisphenoid in mutants with cleft lip only vs. mutants with cleft lip and palate. The two sample t-test demonstrated there was a statistically significant difference in basisphenoid's length, BV/TV, and BMD. However, there was no statistical significance in the width of basisphenoid. The results display the difference in mean value and standard deviation.

Table 3.3: Basisphenoid Comparison between Mutant with Cleft Lip vs. Mutant with Cleft Lip and Palate

Basisphenoid	Genotype	Mean	Std. Dev.	95% Conf. Interval		P-Value
Width	CL	1.22375	.0187861	1.193857	1.253643	0.8937
	CL+P	1.277	.0763675	.5908649	1.963135	
Length	CL	.626	.0107083	.6089608	.6430392	0.0455*
	CL+P	.574	.0509117	.1165766	1.031423	
BV/TV (%)	CL	.3393	.0331487	.2865531	.3920469	0.0313*
	CL+P	.27195	.0197283	.0946984	.4492016	
Actual Density (BMD) (g/cm^2)	CL	1.557825	.0348451	1.502379	1.613271	0.0085*
	CL+P	1.4395	.0340825	1.13328	1.74572	

In Table 3.4, t-test is applied to assess the ratio of Basisphenoid width and Basioccipital width between mutants with cleft lip only vs. mutants with cleft lip and palate. Since Basioccipital development is not affected by *Prickle1* mutation, it served as a good basis for comparison. The two sample t-test demonstrated there was no statistically significant difference in the ratio of Basisphenoid and Basioccipital between the two groups. Therefore, we can estimate that growth potential for all the mutant samples were similar.

Table 3.4: Ratio of Basisphenoid/Basioccipital Width Comparison between Mutant with Cleft Lip vs. Mutant with Cleft Lip and Palate

Phenotype	Mean	Std. Dev.	95% Conf. Interval		P-Value
CL	1.465416	.0233055	1.428332	1.502501	0.3913
CL/P	1.419534	.1026975	.4968341	2.342235	

3.4 TREND IN PHENOTYPE

In order to evaluate possible trend in basisphenoid's dimension and density, mice are analyzed and compared in three different groups: Phenotype 0 = Wild type (no cleft), Phenotype 1 = Mutant with cleft lip only, and Phenotype 3 = Mutant with cleft lip and palate.

Table 3.5: Linear Regression Analysis of Phenotype with Basisphenoid Measurements

Basisphenoid	Regression Coef.	SE	P-Value	Adjusted R^2
Width BS (mm)	.0896786	.0170502	0.001*	0.7476
Length BS (mm)	-.0515714	.0153057	0.010*	0.5350
BV/TV (%)	-.0653929	.0102282	0.000*	0.8159
Actual Density (BMD) (g/cm2)	-.1107393	.0114029	0.000*	0.9120

SE = Standard error

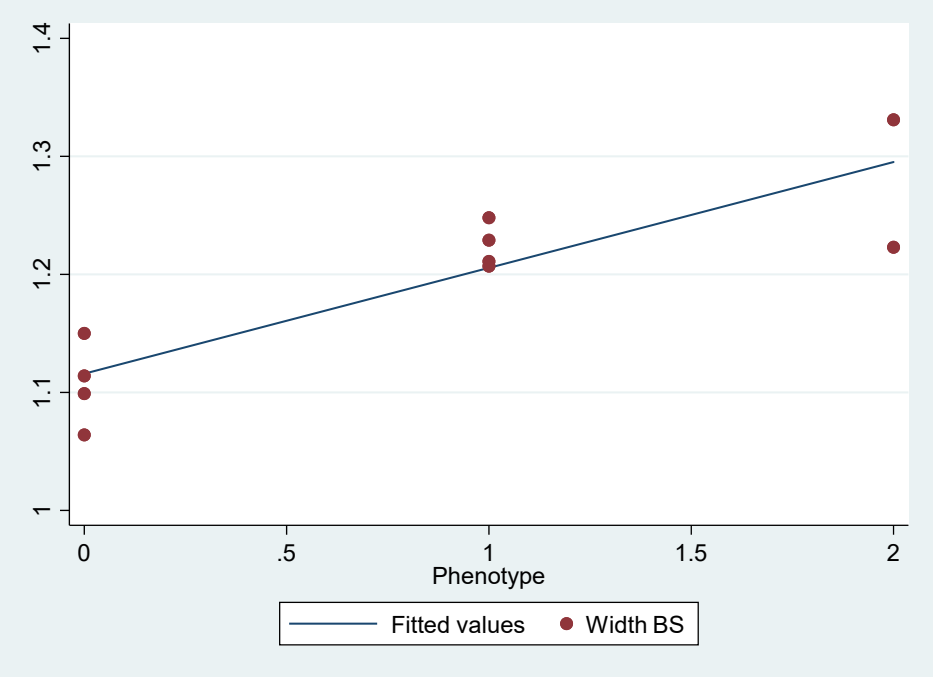

Figure 3.5 Scatter Plot with a fitted line Width of Basisphenoid vs. Phenotype. Phenotype 0 = wild type, Phenotype 1 = Mutant with cleft lip only, Phenotype 2 = Mutant with cleft lip and palate

In Figure 3.4, one can generalize that width of basisphenoid widens as the degree of phenotype progresses. A linear regression in Table 3.4 established that for every unit increase in phenotype, there is .09 increase in width of Basisphenoid. The relationship is statistically significant (p=0.001) and accounts for 74% of the variability in phenotype.

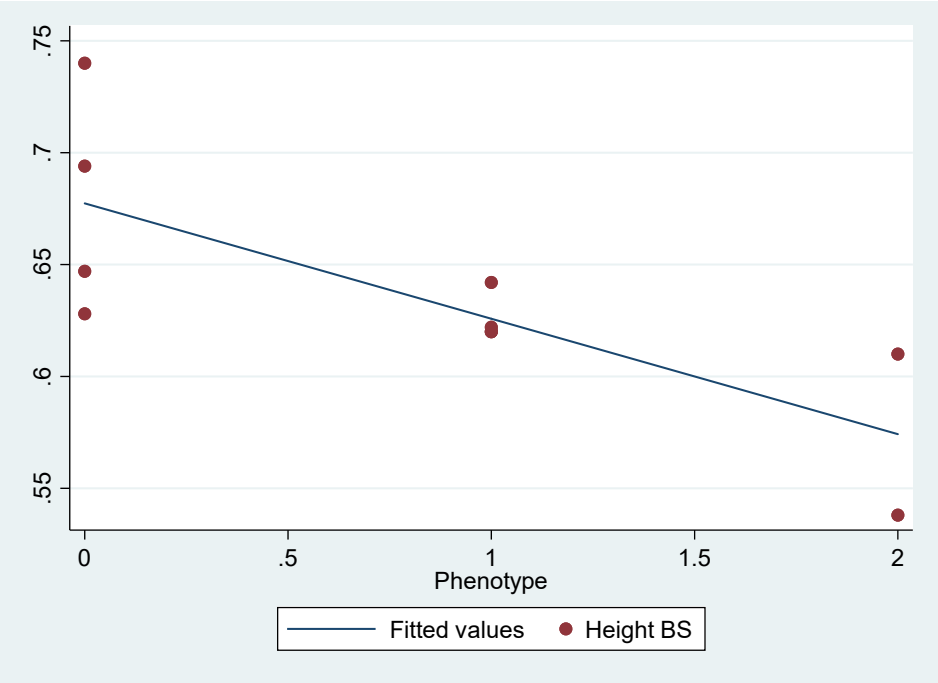

Figure 3.6 Scatter Plot with a fitted line Length of Basisphenoid vs. Phenotype

In Figure 3.5, length of basisphenoid progressively gets shorter from wild type to cleft lip, and cleft lip and palate. Linear regression analysis in Table 3.4 shows that with every increase in phenotype, there is a statistically significant decrease in .05 of basisphenoid length, p=0.01. Basisphenoid length accounts for 53% of the variability in phenotype.

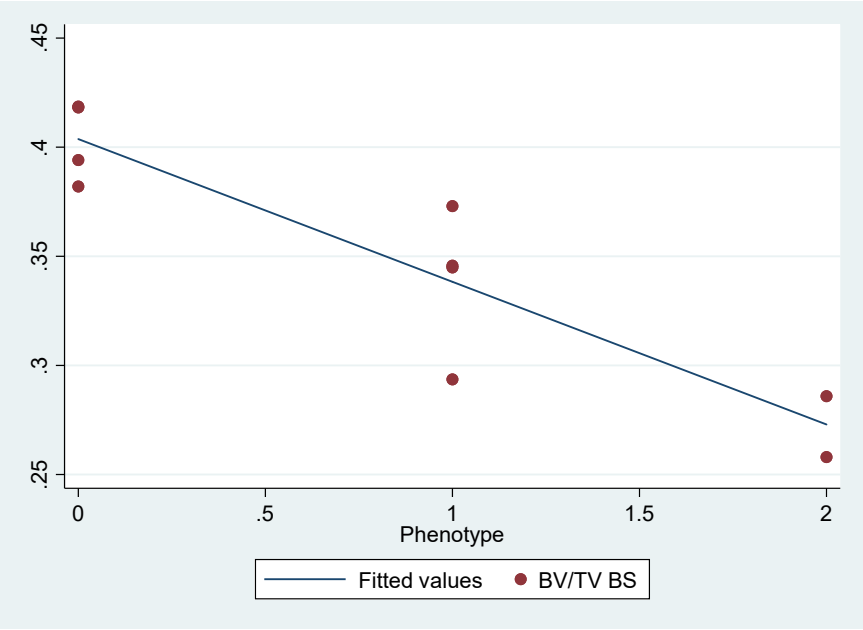

Figure 3.7 Scatter Plot with a fitted line BV/TV of Basisphenoid vs. Phenotype

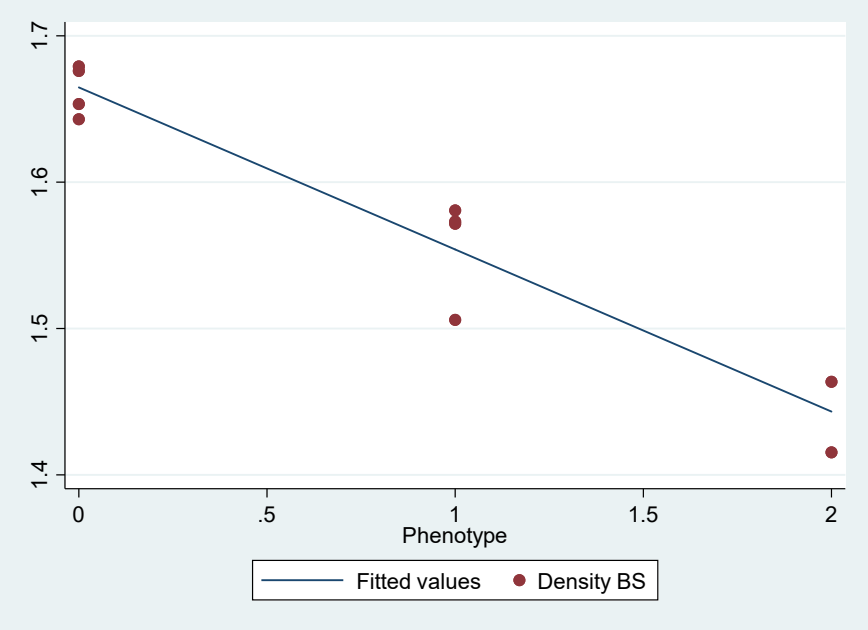

Figure 3.8 Scatter Plot with a fitted line Density of Basisphenoid (BMD) vs. Phenotype

In Figure 3.6 and Figure 3.7, a similar trend is observed in BV/TV and Density of basisphenoid. They both have the highest value in wild type, lower value in mutant with cleft lip only, and the lowest value in mutant with both cleft lip and palate. Table 3.4 indicates that with every unit increase in phenotype results in statistically significant decrease of BV/TV by 0.07 and BMD by .11, p=000. BV/TV accounts for 82% and BMD 92% for the variability in phenotype.

3.5 CELL POLARITY

The basisphenoid bone develops through endochondral ossification which relies heavily on cells maturation and organization into columns. When there is adequate alignment, cells can drive elongation in the AP axis (Shindo et al 2018). My hypothesis is that the orientation of cell division would be different between *Prickle1*$^{Bj/Bj}$ and *Prickle1*$^{+/+}$ in the basisphenoid condensations. To test the hypothesis, we labelled the proliferating cells using bromo-deoxyuridine (BrdU). BrdU is incorporated into cells during S-phasse of the cell cycle as a thymidine analog. We performed a 1-hour pulse labelling of the embryos prior to collection, and performed immunoflourescence labelling using anti-BrdU antibody. The concentration, and dose of the BrdU allows us to determine the location of the daughter cells after division. To analyze the angle of division, we oriented the tissue sections so the proximal region of the cranial base is on the left of the image. After locating daughter cells in close proximity, we measured the angle between them using the program Image J. Data is presented in a radar plot and histogram and reveals that *Prickle1*$^{+/+}$ cells have a preferential dividing angle between 137° to 172° while *Prickle1*$^{Bj/Bj}$ cells divided in a wide-ranging angle from 28° to 176°. Result signifies that *Prickle1*$^{Bj/Bj}$ lacks the ability to orient cells in a linear fashion upon division.

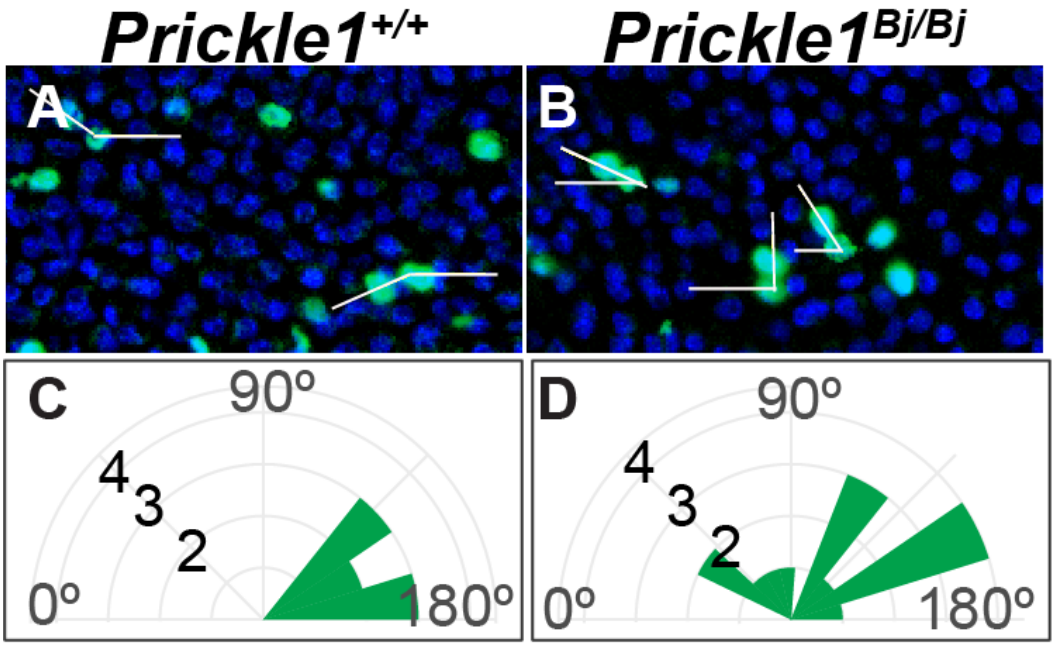

Figure 3.9 Cell Polarity Angles

A) DAPI and BrdU staining of wild type B) DAPI and BrdU staining of mutant C-D) Poly graph of cell polarity angles. Left figure is of wild type with a strong angle bias towards 137 degrees to 172 degrees. Right figure is of mutant displaying varied angles from 28 degrees to 176 degrees.

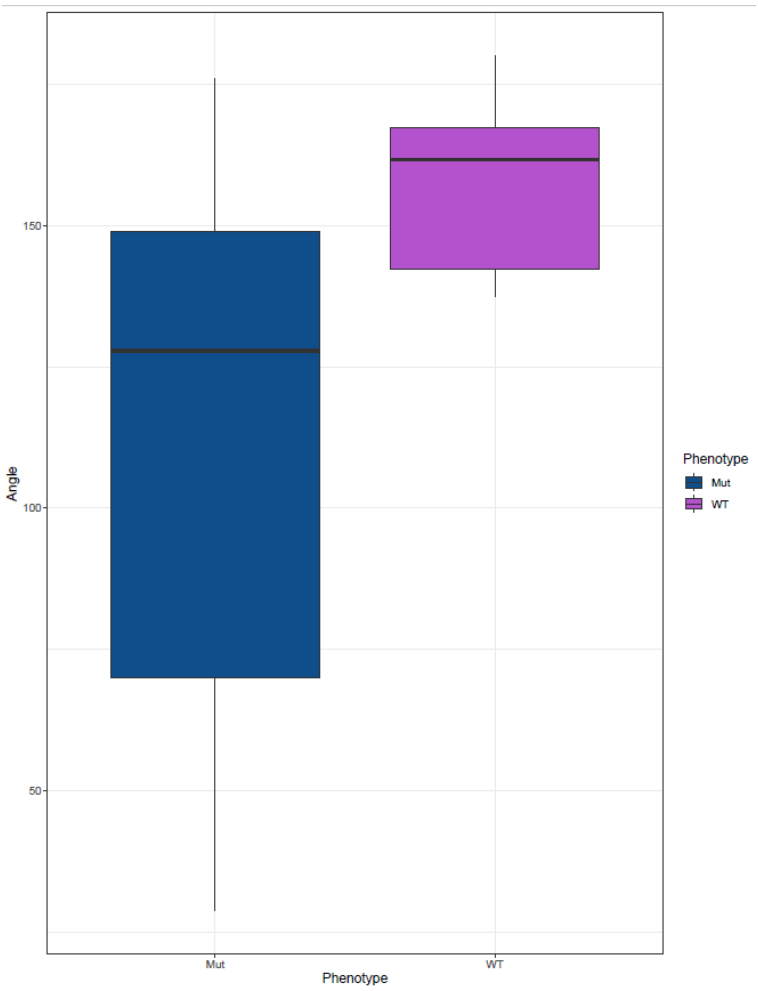

Figure 3.10 Poly histogram of cell polarity angle. Mutant is on the left column with a wide range of cell polarity. It indicates that cell polarity is disrupted, and cells are not properly aligned. Wild type is on the right column with a narrow range of cell polarity, confirming that wild type cells are able to organize and polarize in a conformed direction.

4.0 DISCUSSION

In this study we have found that *Prickle1* is a vital component in basisphenoid bone development and it has association with orofacial cleft. *Prickle1* plays a crucial role in cranial NCCs both during EMT and migration (Ahsan et al 2019), and consequently it has affected development of neural crest origin bone, basisphenoid. The basioccipital bone is of mesodermal origin and is reflected on the insignificant developmental difference between control vs. mutant. Our data has shown that *Prickle1* mutants have basisphenoid with wider width ($p=0.0027$), shorter length ($p=0.0499$), decreased BV/TV ($p=0.0080$), and lower BMD ($p=0.0031$).

The width of basisphenoid may be wider in mutants due to defective chondrocyte stacking. According to Rochard et al, normal chondrocytes orient perpendicularly to the anterioposterior (AP) axis as a single layer. When Wnt pathway is interrupted, chondrocytes were smaller, rounded, and lacked stacking in linear columns. Cells were randomly oriented and exhibited excessive stacking in the dorsoventral (DV) axis (Rochard et al 2016). This phenomenon is evident in our data Figure 4.1. Cellular polarity angle measured in mutants varied greatly from 28° to 176° while wild type cells had preferential angles between 137° to 172°. Thus, we can confirm that when PCP/Wnt pathway is disrupted, chondrocytes cannot orient and stack in an orderly fashion. This may be one of the critical reasons as to why mutants have wider and shorter Basisphenoid.

The basicranium serves as the template that establishes the shape and perimeter of the facial growth field (Enlow et al 2008), and consequently a wide basicranium would create a bigger distance for lateral prominences and palatal shelves to travel before fusing at the midline.

Especially with defective chondrocyte orientation, the risk of orofacial cleft increases dramatically.

Our initial hypothesis was that the width of basisphenoid correlated with the severity of orofacial cleft. However, there was no statistical significance in basisphenoid width between mutants with cleft lip only vs. mutants with cleft lip and palate. Even when it was compared in ratio with basioccipital, there was no statistically significant difference between the two groups. Therefore, we can conclude that the width of cranial base is not a factor in causing cleft palate. However, this study lacks number of samples. Another study should be conducted with more cleft lip and palate samples.

Mutant basisphenoid had lower bone density when compared with control basisphenoid. One reason may be, as Wan et al stated, osteoblast differentiation and maturation by E 16.5 are delayed in *Prickle1*$^{Bj/Bj}$ mutants (Wan et al 2018, 2019). Osteoblasts being the key cells that secrete the matrix for bone formation, its delayed maturation would be a logical reason as to why there is less bone density in mutant basisphenoid.

Another reason for decreased basisphenoid density is that mutants with defective Wnt pathway have chondrocytes that cannot intercalate well with each other. In Wntless protein (Wls) defective mutants, cells remain aggregated throughout the palate, chondrocytes do not intercalate with neighboring cells, and cells extend in both AP and DV axis (Rochard et al 2016). These findings explain why mutants in Figures 3.1.D and F seem much more porous than wild types. Lack of intercalation can be observed in Figure 3.1.F as mutant's basisphenoid fail to converge in the sagittal axis. Literature review suggests that decreased basisphenoid density is from

delayed osteoblast maturation and futile chondrocyte intercalation, convergence and extension causing porosity and midline aperture.

Density of basisphenoid was found to be statistically significant and different between all three groups: wild type, mutants with cleft lip only, and mutants with cleft lip and palate. The general trend showed highest density in wild type and gradual decrease in each group. In this study, density of basisphenoid proved to be the most significant factor associated with the degree of orofacial cleft.

In conclusion, basisphenoid width can be served as a good indicator of orofacial cleft. However, the density of basisphenoid is a superior value in predicting the severity of orofacial cleft.

4.1 FUTURE STUDY:

This study only analyzed a small sample of cleft lip and palate mutants. Further studies with increased sample size would be more promising. A genetic engineering study of *PK1* missense allele may disclose new, helpful information.

5.0 CONCLUSION

In summary, *Prickle1*$^{Bj/Bj}$ mutants have shorter and wider basisphenoid compared to control. Basioccipital dimensions remain unchanged between the two groups. It is evident that mice with wide basisphenoid have greater tendency to develop orofacial cleft, either with cleft lip only or with both cleft lip and palate. Defective *Prickle1* deters chondrocytes from properly orienting and stacking, contributing to the development of a wide cranial base. A wide basal cranium increases distance for palate and lateral prominences to meet at the midline, leading to a higher chance of orofacial cleft. The width of basisphenoid between cleft lip mutant vs. cleft lip and palate mutant was not statistically different. However, the density of basisphenoid was significantly lower for mutants with complete lip and palatal cleft compared to other groups. We can conclude that *Prickle1* is an important component in osteoblast differentiation and chondrocyte intercalation, and a low basisphenoid density is a significant indicator of developing both cleft lip and palate.

APPENDIX

RAW DATA

Table A.1: Sample Genotype and Phenotype

Sample	Genotype	Phenotype
E5	Mutant	Cleft L
E8	Wild Type	
B1	Mutant	Cleft L+P
B4	Wild Type	
B5	Wild Type	
B8	Mutant	Cleft L
B9	Mutant	Cleft L
C2	Mutant	Cleft L
C7	Mutant	Cleft L + P
C8	Wild Type	

Table A.2: Width, Length, BV/TV, and BMD of Basisphenoid bone.

Basisphenoid	Width (mm)	Length (mm)	BV/TV (%)	BMD (mm^3)
E5 Mut	1.207	.642	.2991	1.4174s
E8 WT	1.099	.694	.4026	1.6394
B1 Mut	1.223	.610	.269	1.4887
B4 WT	1.114	.628	.4072	1.6595
B5 WT	1.064	.647	.3659	1.6063
B8 Mut	1.248	.620	.355	1.5826
B9 Mut	1.211	.622	.3022	1.5263
C2 Mut	1.229	.620	.3449	1.5807
C7 Mut	1.331	.538	.2859	1.4154
C8 WT	1.150	.740	.3941	1.6534

Table A.3: Width, length, BV/TV, and BMD of Basioccipital bone

Basioccipital	Width (mm)	Length (mm)	BV/TV (%)	BMD (mm^3)
E5 Mut	.817	1.559	.3275	1.4761
E8 WT	.851	1.485	.4268	1.7945
B1 Mut	.908	1.530	.336	1.6158
B4 WT	.788	1.381	.4161	1.7793
B5 WT	.873	1.690	.3909	1.7374
B8 Mut	.859	1.559	.4166	1.7502
B9 Mut	.841	1.583	.3851	1.6983
C2 Mut	.824	1.657	.4019	1.7441
C7 Mut	.892	1.667	.4077	1.7275
C8 WT	.920	1.541	.4109	1.787

Table A.4: Cell Polarity Angles

Sample	Side	Genotype	Angle
B1 #15	Left	Mutant	149.683
B1 #15	Left	Mutant	152.858
B1 #15	Left	Mutant	128.016
B1 #15	Left	Mutant	176.055
B1 #15	Right	Mutant	127.694
B1 #15	Right	Mutant	29.745
B1 #15	Right	Mutant	63.435
B1 #15	Right	Mutant	151.316
B1 #10	Left	Mutant	113.05
B1 #10	Left	Mutant	133.731
B1 #10	Left	Mutant	146.31
B1 #10	Right	Mutant	28.782
B1 #10	Right	Mutant	90
B1 #10	Right	Mutant	59.036
B1 #10	Left	Wild Type	180
B1 #10	Left	Wild Type	143.569
B1 #10	Left	Wild Type	161.822
B1 #10	Right	Wild Type	172.439
B1 #10	Right	Wild Type	138.174
B1 #15	Left	Wild Type	137.428
B1 #15	Left	Wild Type	161.359
B1 #15	Right	Wild Type	165.674

BIBLIOGRAPHY

1. Ahsan K, Singh N, Rocha M, Huang C, Prince VE. Prickle1 is required for EMT and migration of zebrafish cranial neural crest. Dev Biol 2019;448(1):16-35.
2. Axelrod JD, Bergmann DC. Coordinating cell polarity: heading in the right direction? Development 2014;141(17):3298-302.
3. Brinkley LL, Morris-Wiman J. The role of extracellular matrices in palatal shelf closure. Curr Top Dev Biol 1984;19:17-36.
4. Bush JO, Jiang R. Palatogenesis: morphogenetic and molecular mechanisms of secondary palate development. Development 2012;139(2):231-43.
5. Chazotte B. Labeling nuclear DNA using DAPI. Cold Spring Harb Protoc 2011;2011(1):pdb prot5556.
6. Christensen K, Juel K, Herskind AM, Murray JC. Long term follow up study of survival associated with cleft lip and palate at birth. BMJ 2004;328(7453):1405.
7. Cui C, Chatterjee B, Lozito TP, et al. Wdpcp, a PCP protein required for ciliogenesis, regulates directional cell migration and cell polarity by direct modulation of the actin cytoskeleton. PLoS Biol 2013;11(11):e1001720.
8. Devenport D. The cell biology of planar cell polarity. J Cell Biol 2014;207(2):171-9.
9. Ding R, Tsunekawa N, Obata K. Cleft palate by picrotoxin or 3-MP and palatal shelf elevation in GABA-deficient mice. Neurotoxicol Teratol 2004;26(4):587-92.
10. Dixon MJ, Marazita ML, Beaty TH, Murray JC. Cleft lip and palate: understanding genetic and environmental influences. Nat Rev Genet 2011;12(3):167-78.
11. Enlow DH, Hans MG. Essentials of facial growth. 2nd ed. Ann Arbor, MI: Distributed by Needham Press; 2008.
12. Ferguson MW. Palate development. Development 1988;103 Suppl:41-60.
13. Ferros I, Mora MJ, Obeso IF, Jimenez P, Martinez-Insua A. The nasomaxillary complex and the cranial base in artificial cranial deformation: relationships from a geometric morphometric study. Eur J Orthod 2015;37(4):403-11.
14. Franco FC, de Araujo TM, Vogel CJ, Quintao CC. Brachycephalic, dolichocephalic and mesocephalic: Is it appropriate to describe the face using skull patterns? Dental Press J Orthod 2013;18(3):159-63.
15. Gao Y, Lan Y, Ovitt CE, Jiang R. Functional equivalence of the zinc finger transcription factors Osr1 and Osr2 in mouse development. Dev Biol 2009;328(2):200-9.
16. Gibbs BC, Damerla RR, Vladar EK, et al. Prickle1 mutation causes planar cell polarity and directional cell migration defects associated with cardiac outflow tract anomalies and other structural birth defects. Biol Open 2016;5(3):323-35.
17. Grosen D, Chevrier C, Skytthe A, et al. A cohort study of recurrence patterns among more than 54,000 relatives of oral cleft cases in Denmark: support for the multifactorial threshold model of inheritance. J Med Genet 2010;47(3):162-8.
18. Honein MA, Rasmussen SA, Reefhuis J, et al. Maternal smoking and environmental tobacco smoke exposure and the risk of orofacial clefts. Epidemiology 2007;18(2):226-33.
19. Kaartinen V, Voncken JW, Shuler C, et al. Abnormal lung development and cleft palate in mice lacking TGF-beta 3 indicates defects of epithelial-mesenchymal interaction. Nat Genet 1995;11(4):415-21.
20. Kist R, Greally E, Peters H. Derivation of a mouse model for conditional inactivation of Pax9. Genesis 2007;45(7):460-4.

21. Little J, Cardy A, Munger RG. Tobacco smoking and oral clefts: a meta-analysis. Bull World Health Organ 2004;82(3):213-8.
22. McBratney-Owen B, Iseki S, Bamforth SD, Olsen BR, Morriss-Kay GM. Development and tissue origins of the mammalian cranial base. Dev Biol 2008;322(1):121-32.
23. Miettinen PJ, Chin JR, Shum L, et al. Epidermal growth factor receptor function is necessary for normal craniofacial development and palate closure. Nat Genet 1999;22(1):69-73.
24. Minoux M, Rijli FM. Molecular mechanisms of cranial neural crest cell migration and patterning in craniofacial development. Development 2010;137(16):2605-21.
25. Mori-Akiyama Y, Akiyama H, Rowitch DH, de Crombrugghe B. Sox9 is required for determination of the chondrogenic cell lineage in the cranial neural crest. Proc Natl Acad Sci U S A 2003;100(16):9360-5.
26. Murray JC, Schutte BC. Cleft palate: players, pathways, and pursuits. J Clin Invest 2004;113(12):1676-8.
27. Natsume N, Kato T, Hayakawa T, Imura H. Diagnostic/genetic sreening - approach for genetic diagnoses and prevention of cleft lip and/or palate. Chin J Dent Res 2013;16(2):95-100.
28. Nawshad A. Palatal seam disintegration: to die or not to die? that is no longer the question. Dev Dyn 2008;237(10):2643-56.
29. Nawshad A, LaGamba D, Hay ED. Transforming growth factor beta (TGFbeta) signalling in palatal growth, apoptosis and epithelial mesenchymal transformation (EMT). Arch Oral Biol 2004;49(9):675-89.
30. Panamonta V, Pradubwong S, Panamonta M, Chowchuen B. Global Birth Prevalence of Orofacial Clefts: A Systematic Review. J Med Assoc Thai 2015;98 Suppl 7:S11-21.
31. Parker SE, Mai CT, Canfield MA, et al. Updated National Birth Prevalence estimates for selected birth defects in the United States, 2004-2006. Birth Defects Res A Clin Mol Teratol 2010;88(12):1008-16.
32. Proffit WR, Fields HW, Sarver DM. Contemporary orthodontics. 4th ed. St. Louis, Mo.: Mosby Elsevier; 2007.
33. Rice R, Spencer-Dene B, Connor EC, et al. Disruption of Fgf10/Fgfr2b-coordinated epithelial-mesenchymal interactions causes cleft palate. J Clin Invest 2004;113(12):1692-700.
34. Rochard L, Monica SD, Ling IT, et al. Roles of Wnt pathway genes wls, wnt9a, wnt5b, frzb and gpc4 in regulating convergent-extension during zebrafish palate morphogenesis. Development 2016;143(14):2541-7.
35. St Louis AM, Kim K, Browne ML, et al. Prevalence trends of selected major birth defects: A multi-state population-based retrospective study, United States, 1999 to 2007. Birth Defects Res 2017;109(18):1442-50.
36. Szeto DP, Rodriguez-Esteban C, Ryan AK, et al. Role of the Bicoid-related homeodomain factor Pitx1 in specifying hindlimb morphogenesis and pituitary development. Genes Dev 1999;13(4):484-94.
37. Theveneau E, Mayor R. Neural crest migration: interplay between chemorepellents, chemoattractants, contact inhibition, epithelial-mesenchymal transition, and collective cell migration. Wiley Interdiscip Rev Dev Biol 2012;1(3):435-45.
38. Vladar EK, Antic D, Axelrod JD. Planar cell polarity signaling: the developing cell's compass. Cold Spring Harb Perspect Biol 2009;1(3):a002964.
39. Wan Y, Lantz B, Cusack BJ, Szabo-Rogers HL. Prickle1 regulates differentiation of frontal bone osteoblasts. Sci Rep 2018;8(1):18021.
40. Yazdy MM, Autry AR, Honein MA, Frias JL. Use of special education services by children with orofacial clefts. Birth Defects Res A Clin Mol Teratol 2008;82(3):147-54.

41. Yu L, Gu S, Alappat S, et al. Shox2-deficient mice exhibit a rare type of incomplete clefting of the secondary palate. Development 2005;132(19):4397-406.
42. Zhang L, Li H, Zeng S, et al. Long-term tracing of the BrdU label-retaining cells in adult rat brain. Neurosci Lett 2015;591:30-4.